Measurement and interpretation of fermion-pair production at LEP energies of 183 and 189 GeV

DELPHI Collaboration

P. Abreu [u], W. Adam [ay], T. Adye [ak], P. Adzic [k], Z. Albrecht [q], T. Alderweireld [b],
G.D. Alekseev [p], R. Alemany [ax], T. Allmendinger [q], P.P. Allport [v], S. Almehed [x],
U. Amaldi [ab], N. Amapane [at], S. Amato [av], E.G. Anassontzis [c], P. Andersson [as],
A. Andreazza [aa], S. Andringa [u], P. Antilogus [y], W-D. Apel [q], Y. Arnoud [n],
B. Åsman [as], J-E. Augustin [w], A. Augustinus [i], P. Baillon [i], A. Ballestrero [at],
P. Bambade [i,s], F. Barao [u], G. Barbiellini [au], R. Barbier [y], D.Y. Bardin [p], G. Barker [q],
A. Baroncelli [am], M. Battaglia [o], M. Baubillier [w], K-H. Becks [ba], M. Begalli [f],
A. Behrmann [ba], P. Beilliere [h], Yu. Belokopytov [i], K. Belous [aq], N.C. Benekos [af],
A.C. Benvenuti [e], C. Berat [n], M. Berggren [w], L. Berntzon [as], D. Bertrand [b],
M. Besancon [an], M.S. Bilenky [p], M-A. Bizouard [s], D. Bloch [j], H.M. Blom [ae],
M. Bonesini [ab], M. Boonekamp [an], P.S.L. Booth [v], G. Borisov [s], C. Bosio [ap],
O. Botner [aw], E. Boudinov [ae], B. Bouquet [s], C. Bourdarios [s], T.J.V. Bowcock [v],
I. Boyko [p], I. Bozovic [k], M. Bozzo [m], M. Bracko [ar], P. Branchini [am], R.A. Brenner [aw],
P. Bruckman [i], J-M. Brunet [h], L. Bugge [ag], T. Buran [ag], B. Buschbeck [ay],
P. Buschmann [ba], S. Cabrera [ax], M. Caccia [aa], M. Calvi [ab], T. Camporesi [i], V. Canale [al],
F. Carena [i], L. Carroll [v], C. Caso [m], M.V. Castillo Gimenez [ax], A. Cattai [i],
F.R. Cavallo [e], M. Chapkin [aq], Ph. Charpentier [i], P. Checchia [aj], G.A. Chelkov [p],
R. Chierici [at], P. Chliapnikov [i,aq], P. Chochula [g], V. Chorowicz [y], J. Chudoba [ad],
K. Cieslik [r], P. Collins [i], R. Contri [m], E. Cortina [ax], G. Cosme [s], F. Cossutti [i],
M. Costa [ax], H.B. Crawley [a], D. Crennell [ak], G. Crosetti [m], J. Cuevas Maestro [ah],
S. Czellar [o], J. D'Hondt [b], J. Dalmau [as], M. Davenport [i], W. Da Silva [w],
G. Della Ricca [au], P. Delpierre [z], N. Demaria [at], A. De Angelis [au], W. De Boer [q],
C. De Clercq [b], B. De Lotto [au], A. De Min [i], L. De Paula [av], H. Dijkstra [i],
L. Di Ciaccio [al], J. Dolbeau [h], K. Doroba [az], M. Dracos [j], J. Drees [ba], M. Dris [af],
G. Eigen [d], T. Ekelof [aw], M. Ellert [aw], M. Elsing [i], J-P. Engel [j], M. Espirito Santo [i],
G. Fanourakis [k], D. Fassouliotis [k], M. Feindt [q], J. Fernandez [ao], A. Ferrer [ax],

E. Ferrer-Ribas [s], F. Ferro [m], A. Firestone [a], U. Flagmeyer [ba], H. Foeth [i], E. Fokitis [af],
F. Fontanelli [m], B. Franek [ak], A.G. Frodesen [d], R. Fruhwirth [ay], F. Fulda-Quenzer [s],
J. Fuster [ax], A. Galloni [v], D. Gamba [at], S. Gamblin [s], M. Gandelman [av], C. Garcia [ax],
C. Gaspar [i], M. Gaspar [av], U. Gasparini [aj], Ph. Gavillet [i], E.N. Gazis [af], D. Gele [j],
T. Geralis [k], N. Ghodbane [y], I. Gil [ax], F. Glege [ba], R. Gokieli [i,az], B. Golob [i,ar],
G. Gomez-Ceballos [ao], P. Goncalves [u], I. Gonzalez Caballero [ao], G. Gopal [ak], L. Gorn [a],
Yu. Gouz [aq], V. Gracco [m], J. Grahl [a], E. Graziani [am], P. Gris [an], G. Grosdidier [s],
K. Grzelak [az], J. Guy [ak], C. Haag [q], F. Hahn [i], S. Hahn [ba], S. Haider [i], A. Hallgren [aw],
K. Hamacher [ba], J. Hansen [ag], F.J. Harris [ai], F. Hauler [q], V. Hedberg [i,x], S. Heising [q],
J.J. Hernandez [ax], P. Herquet [b], H. Herr [i], E. Higon [ax], S-O. Holmgren [as], P.J. Holt [ai],
S. Hoorelbeke [b], M. Houlden [v], J. Hrubec [ay], M. Huber [q], G.J. Hughes [v],
K. Hultqvist [i,as], J.N. Jackson [v], R. Jacobsson [i], P. Jalocha [r], R. Janik [g], Ch. Jarlskog [x],
G. Jarlskog [x], P. Jarry [an], B. Jean-Marie [s], D. Jeans [ai], E.K. Johansson [as], P. Jonsson [y],
C. Joram [i], P. Juillot [j], L. Jungermann [q], F. Kapusta [w], K. Karafasoulis [k],
S. Katsanevas [y], E.C. Katsoufis [af], R. Keranen [q], G. Kernel [ar], B.P. Kersevan [ar],
Yu. Khokhlov [aq], B.A. Khomenko [p], N.N. Khovanski [p], A. Kiiskinen [o], B. King [v],
A. Kinvig [v], N.J. Kjaer [i], O. Klapp [ba], P. Kluit [ae], P. Kokkinias [k], V. Kostioukhine [aq],
C. Kourkoumelis [c], O. Kouznetsov [p], M. Krammer [ay], E. Kriznic [ar], Z. Krumstein [p],
P. Kubinec [g], J. Kurowska [az], K. Kurvinen [o], J.W. Lamsa [a], D.W. Lane [a], V. Lapin [aq],
J-P. Laugier [an], R. Lauhakangas [o], G. Leder [ay], F. Ledroit [n], L. Leinonen [as], A. Leisos [k],
R. Leitner [ad], J. Lemonne [b], G. Lenzen [ba], V. Lepeltier [s], T. Lesiak [r], M. Lethuillier [y],
J. Libby [ai], W. Liebig [ba], D. Liko [i], A. Lipniacka [as], I. Lippi [aj], B. Loerstad [x],
J.G. Loken [ai], J.H. Lopes [av], J.M. Lopez [ao], R. Lopez-Fernandez [n], D. Loukas [k],
P. Lutz [an], L. Lyons [ai], J. MacNaughton [ay], J.R. Mahon [f], A. Maio [u], A. Malek [ba],
S. Maltezos [af], V. Malychev [p], F. Mandl [ay], J. Marco [ao], R. Marco [ao], B. Marechal [av],
M. Margoni [aj], J-C. Marin [i], C. Mariotti [i], A. Markou [k], C. Martinez-Rivero [i],
S. Marti i Garcia [i], J. Masik [l], N. Mastroyiannopoulos [k], F. Matorras [ao],
C. Matteuzzi [ab], G. Matthiae [al], F. Mazzucato [aj], M. Mazzucato [aj], M. Mc Cubbin [v],
R. Mc Kay [a], R. Mc Nulty [v], G. Mc Pherson [v], E. Merle [n], C. Meroni [aa],
W.T. Meyer [a], A. Miagkov [aq], E. Migliore [i], L. Mirabito [y], W.A. Mitaroff [ay],
U. Mjoernmark [x], T. Moa [as], M. Moch [q], R. Moeller [ac], K. Moenig [i,l], M.R. Monge [m],
D. Moraes [av], P. Morettini [m], G. Morton [ai], U. Mueller [ba], K. Muenich [ba], M. Mulders [ae],
C. Mulet-Marquis [n], L.M. Mundim [f], R. Muresan [x], W.J. Murray [ak], B. Muryn [r],
G. Myatt [ai], T. Myklebust [ag], F. Naraghi [n], M. Nassiakou [k], F.L. Navarria [e],
K. Nawrocki [az], P. Negri [ab], N. Neufeld [ay], R. Nicolaidou [an], B.S. Nielsen [ac],
P. Niezurawski [az], M. Nikolenko [j,p], V. Nomokonov [o], A. Nygren [x], V. Obraztsov [aq],
A.G. Olshevski [p], A. Onofre [u], R. Orava [o], G. Orazi [j], K. Osterberg [i], A. Ouraou [an],

A. Oyanguren [ax], M. Paganoni [ab], S. Paiano [e], R. Pain [w], R. Paiva [u], J. Palacios [ai],
H. Palka [r], Th.D. Papadopoulou [af], L. Pape [i], C. Parkes [i], F. Parodi [m], U. Parzefall [v],
A. Passeri [am], O. Passon [ba], T. Pavel [x], M. Pegoraro [aj], L. Peralta [u], M. Pernicka [ay],
A. Perrotta [e], C. Petridou [au], A. Petrolini [m], H.T. Phillips [ak], F. Pierre [an], M. Pimenta [u],
E. Piotto [aa], T. Podobnik [ar], V. Poireau [an], M.E. Pol [f], G. Polok [r], P. Poropat [au],
V. Pozdniakov [p], P. Privitera [al], N. Pukhaeva [p], A. Pullia [ab], D. Radojicic [ai],
S. Ragazzi [ab], H. Rahmani [af], J. Rames [l], P.N. Ratoff [t], A.L. Read [ag], P. Rebecchi [i],
N.G. Redaelli [ab], M. Regler [ay], J. Rehn [q], D. Reid [ae], P. Reinertsen [d], R. Reinhardt [ba],
P.B. Renton [ai], L.K. Resvanis [c], F. Richard [s], J. Ridky [l], G. Rinaudo [at],
I. Ripp-Baudot [j], A. Romero [at], P. Ronchese [aj], E.I. Rosenberg [a], P. Rosinsky [g],
P. Roudeau [s], T. Rovelli [e], V. Ruhlmann-Kleider [an], A. Ruiz [ao], H. Saarikko [o],
Y. Sacquin [an], A. Sadovsky [p], G. Sajot [n], J. Salt [ax], D. Sampsonidis [k], M. Sannino [m],
A. Savoy-Navarro [w], Ph. Schwemling [w], B. Schwering [ba], U. Schwickerath [q],
F. Scuri [au], P. Seager [t], Y. Sedykh [p], A.M. Segar [ai], N. Seibert [q], R. Sekulin [ak],
G. Sette [m], R.C. Shellard [f], M. Siebel [ba], L. Simard [an], F. Simonetto [aj], A.N. Sisakian [p],
G. Smadja [y], O. Smirnova [x], G.R. Smith [ak], A. Sopczak [q], R. Sosnowski [az],
T. Spassov [i], E. Spiriti [am], S. Squarcia [m], C. Stanescu [am], M. Stanitzki [q],
K. Stevenson [ai], A. Stocchi [s], J. Strauss [ay], R. Strub [j], B. Stugu [d], M. Szczekowski [az],
M. Szeptycka [az], T. Tabarelli [ab], A. Taffard [v], O. Tchikilev [aq], F. Tegenfeldt [aw],
F. Terranova [ab], J. Timmermans [ae], N. Tinti [e], L.G. Tkatchev [p], M. Tobin [v],
S. Todorova [i], B. Tome [u], A. Tonazzo [i], L. Tortora [am], P. Tortosa [ax], G. Transtromer [x],
D. Treille [i], G. Tristram [h], M. Trochimczuk [az], C. Troncon [aa], M-L. Turluer [an],
I.A. Tyapkin [p], P. Tyapkin [x], S. Tzamarias [k], O. Ullaland [i], V. Uvarov [aq], G. Valenti [i,e],
E. Vallazza [au], P. Van Dam [ae], W. Van den Boeck [b], W.K. Van Doninck [b],
J. Van Eldik [i,ae], A. Van Lysebetten [b], N. van Remortel [b], I. Van Vulpen [ae],
G. Vegni [aa], L. Ventura [aj], W. Venus [ak,i], F. Verbeure [b], P. Verdier [y], M. Verlato [aj],
L.S. Vertogradov [p], V. Verzi [aa], D. Vilanova [an], L. Vitale [au], E. Vlasov [aq],
A.S. Vodopyanov [p], G. Voulgaris [c], V. Vrba [l], H. Wahlen [ba], A.J. Washbrook [v],
C. Weiser [i], D. Wicke [i], J.H. Wickens [b], G.R. Wilkinson [ai], M. Winter [j], M. Witek [r],
G. Wolf [i], J. Yi [a], O. Yushchenko [aq], A. Zalewska [r], P. Zalewski [az], D. Zavrtanik [ar],
E. Zevgolatakos [k], N.I. Zimin [p,x], A. Zintchenko [p], Ph. Zoller [j],
G. Zumerle [aj], M. Zupan [k]

[a] *Department of Physics and Astronomy, Iowa State University, Ames, IA 50011-3160, USA*
[b] *Physics Department, Univ. Instelling Antwerpen, Universiteitsplein 1, B-2610 Antwerpen, Belgium,*
and IIHE, ULB-VUB, Pleinlaan 2, B-1050 Brussels, Belgium,
and Faculté des Sciences, Univ. de l'Etat Mons, Av. Maistriau 19, B-7000 Mons, Belgium
[c] *Physics Laboratory, University of Athens, Solonos Str. 104, GR-10680 Athens, Greece*
[d] *Department of Physics, University of Bergen, Allégaten 55, NO-5007 Bergen, Norway*
[e] *Dipartimento di Fisica, Università di Bologna and INFN, Via Irnerio 46, IT-40126 Bologna, Italy*

[f] *Centro Brasileiro de Pesquisas Físicas, rua Xavier Sigaud 150, BR-22290 Rio de Janeiro, Brazil,*
and Depto. de Física, Pont. Univ. Católica, C.P. 38071 BR-22453 Rio de Janeiro, Brazil,
and Inst. de Física, Univ. Estadual do Rio de Janeiro, rua São Francisco Xavier 524, Rio de Janeiro, Brazil
[g] *Comenius University, Faculty of Mathematics and Physics, Mlynska Dolina, SK-84215 Bratislava, Slovakia*
[h] *Collège de France, Lab. de Physique Corpusculaire, IN2P3-CNRS, FR-75231 Paris Cedex 05, France*
[i] *CERN, CH-1211 Geneva 23, Switzerland*
[j] *Institut de Recherches Subatomiques, IN2P3 - CNRS / ULP - BP20, FR-67037 Strasbourg Cedex, France*
[k] *Institute of Nuclear Physics, N.C.S.R. Demokritos, P.O. Box 60228, GR-15310 Athens, Greece*
[l] *FZU, Inst. of Phys. of the C.A.S. High Energy Physics Division, Na Slovance 2, CZ-180 40 Praha 8, Czech Republic*
[m] *Dipartimento di Fisica, Università di Genova and INFN, Via Dodecaneso 33, IT-16146 Genova, Italy*
[n] *Institut des Sciences Nucléaires, IN2P3-CNRS, Université de Grenoble 1, FR-38026 Grenoble Cedex, France*
[o] *Helsinki Institute of Physics, HIP, P.O. Box 9, FI-00014 Helsinki, Finland*
[p] *Joint Institute for Nuclear Research, Dubna, Head Post Office, P.O. Box 79, RU-101 000 Moscow, Russian Federation*
[q] *Institut für Experimentelle Kernphysik, Universität Karlsruhe, Postfach 6980, DE-76128 Karlsruhe, Germany*
[r] *Institute of Nuclear Physics and University of Mining and Metalurgy, Ul. Kawiory 26a, PL-30055 Krakow, Poland*
[s] *Université de Paris-Sud, Lab. de l'Accélérateur Linéaire, IN2P3-CNRS, Bât. 200, FR-91405 Orsay Cedex, France*
[t] *School of Physics and Chemistry, University of Lancaster, Lancaster LA1 4YB, UK*
[u] *LIP, IST, FCUL - Av. Elias Garcia, 14-1°, PT-1000 Lisboa Codex, Portugal*
[v] *Department of Physics, University of Liverpool, P.O. Box 147, Liverpool L69 3BX, UK*
[w] *LPNHE, IN2P3-CNRS, Univ. Paris VI et VII, Tour 33 (RdC), 4 place Jussieu, FR-75252 Paris Cedex 05, France*
[x] *Department of Physics, University of Lund, Sölvegatan 14, SE-223 63 Lund, Sweden*
[y] *Université Claude Bernard de Lyon, IPNL, IN2P3-CNRS, FR-69622 Villeurbanne Cedex, France*
[z] *Univ. d'Aix - Marseille II - CPP, IN2P3-CNRS, FR-13288 Marseille Cedex 09, France*
[aa] *Dipartimento di Fisica, Università di Milano and INFN-MILANO, Via Celoria 16, IT-20133 Milan, Italy*
[ab] *Dipartimento di Fisica, Univ. di Milano-Bicocca and INFN-MILANO, Piazza delle Scienze 2, IT-20126 Milan, Italy*
[ac] *Niels Bohr Institute, Blegdamsvej 17, DK-2100 Copenhagen Ø, Denmark*
[ad] *IPNP of MFF, Charles Univ., Areal MFF, V Holesovickach 2, CZ-180 00 Praha 8, Czech Republic*
[ae] *NIKHEF, Postbus 41882, NL-1009 DB Amsterdam, The Netherlands*
[af] *National Technical University, Physics Department, Zografou Campus, GR-15773 Athens, Greece*
[ag] *Physics Department, University of Oslo, Blindern, NO-1000 Oslo 3, Norway*
[ah] *Dpto. Fisica, Univ. Oviedo, Avda. Calvo Sotelo s / n, ES-33007 Oviedo, Spain*
[ai] *Department of Physics, University of Oxford, Keble Road, Oxford OX1 3RH, UK*
[aj] *Dipartimento di Fisica, Università di Padova and INFN, Via Marzolo 8, IT-35131 Padua, Italy*
[ak] *Rutherford Appleton Laboratory, Chilton, Didcot OX11 OQX, UK*
[al] *Dipartimento di Fisica, Università di Roma II and INFN, Tor Vergata, IT-00173 Rome, Italy*
[am] *Dipartimento di Fisica, Università di Roma III and INFN, Via della Vasca Navale 84, IT-00146 Rome, Italy*
[an] *DAPNIA / Service de Physique des Particules, CEA-Saclay, FR-91191 Gif-sur-Yvette Cedex, France*
[ao] *Instituto de Fisica de Cantabria (CSIC-UC), Avda. los Castros s / n, ES-39006 Santander, Spain*
[ap] *Dipartimento di Fisica, Università degli Studi di Roma La Sapienza, Piazzale Aldo Moro 2, IT-00185 Rome, Italy*
[aq] *Inst. for High Energy Physics, Serpukov P.O. Box 35, Protvino (Moscow Region), Russian Federation*
[ar] *J. Stefan Institute, Jamova 39, SI-1000 Ljubljana, Slovenia*
and Laboratory for Astroparticle Physics, Nova Gorica Polytechnic, Kostanjeviska 16a, SI-5000 Nova Gorica, Slovenia,
and Department of Physics, University of Ljubljana, SI-1000 Ljubljana, Slovenia
[as] *Fysikum, Stockholm University, Box 6730, SE-113 85 Stockholm, Sweden*
[at] *Dipartimento di Fisica Sperimentale, Università di Torino and INFN, Via P. Giuria 1, IT-10125 Turin, Italy*
[au] *Dipartimento di Fisica, Università di Trieste and INFN, Via A. Valerio 2, IT-34127 Trieste, Italy,*
and Istituto di Fisica, Università di Udine, IT-33100 Udine, Italy
[av] *Univ. Federal do Rio de Janeiro, C.P. 68528 Cidade Univ., Ilha do Fundão, BR-21945-970 Rio de Janeiro, Brazil*
[aw] *Department of Radiation Sciences, University of Uppsala, P.O. Box 535, SE-751 21 Uppsala, Sweden*
[ax] *IFIC, Valencia-CSIC, and D.F.A.M.N., U. de Valencia, Avda. Dr. Moliner 50, ES-46100 Burjassot (Valencia), Spain*
[ay] *Institut für Hochenergiephysik, Österr. Akad. d. Wissensch., Nikolsdorfergasse 18, AT-1050 Vienna, Austria*
[az] *Inst. Nuclear Studies and University of Warsaw, Ul. Hoza 69, PL-00681 Warsaw, Poland*
[ba] *Fachbereich Physik, University of Wuppertal, Postfach 100 127, DE-42097 Wuppertal, Germany*

Abstract

An analysis of the data collected in 1997 and 1998 with the DELPHI detector at e^+e^- collision energies close to 183 and 189 GeV was performed in order to extract the hadronic and leptonic fermion-pair cross-sections, as well as the leptonic forward–backward asymmetries and angular distributions. The data are used to put limit on contact interactions between fermions, the exchange of R-parity violating SUSY sneutrinos, Z′ bosons and the existence of gravity in extra dimensions. © 2000 Published by Elsevier Science B.V.

1. Introduction

Results are presented from the analyses of fermion-pair final states collected in 1997 and 1998 by the DELPHI experiment [1] at centre-of-mass energies, $\sqrt{s}$, close to 183 and 189 GeV. Measurements of cross-sections for inclusive hadronic, electron–positron pairs, muon-pair and tau-pair final states are given, together with leptonic forward–backward asymmetries. These results complement those obtained from data collected in 1995 and 1996 at lower collision energies from 130 to 172 GeV [2]. Polar angle distributions of $\mu^+\mu^-$ and $\tau^+\tau^-$ events recorded at $\sqrt{s} \sim 183$ and 189 GeV are also given.

The measurements of the cross-sections and forward–backward asymmetries together with the results presented in [2] and from LEP running in the vicinity of the Z-resonance [3,4], are used to update the searches for new physics involving contact interactions, R-parity violating SUSY, and additional neutral gauge bosons given in [2]. In addition, the measurements presented in this paper are used to search for possible effects of gravity proposed in theories with large extra dimensions.

Results on fermion-pair production at LEP at collision energies from 130 to 189 GeV from the other LEP experiments together with limits derived from these results, can be found in [5].

The measurements of cross-sections, forward–backward asymmetries and angular distributions are given in Section 2. The interpretations of the data are presented in Section 3. A summary and conclusions are given in Section 4. Further details concerning the data analysis, including the event selection and the

theoretical and technical details of the searches for new physics can be found in [2].

2. Measurements of cross-sections and asymmetries

2.1. Luminosity and centre-of-mass energy determination

The luminosity analysis of the data collected during LEP operation in 1997 and 1998 followed closely the one described in [2]. The total experimental systematic uncertainty on the integrated luminosity determination amounts to 0.50%, to be combined with a 0.25% uncertainty reflecting the precision of the theoretical calculations underlying the computation of the cross-section visible in the luminometers. The luminosities for the analysis of the inclusive hadronic final states were 52.80 and 155.21 pb^{-1} for $\sqrt{s} \sim 183$ and 189 GeV respectively. Estimates of the mean centre-of-mass energies led to values of (182.65 ± 0.05) and (188.63 ± 0.05) GeV [6]. There are small differences in the luminosities and mean centre-of-mass energies for the other channels due to the selection of different running periods for analysis, based on the performance of the subdetectors of DELPHI.

2.2. Kinematical definition of signal

Cross-sections and forward–backward asymmetry measurements are given for different ranges of the reduced centre-of-mass energy, $\sqrt{s'}$: for hadronic final states an *inclusive* sample, $\sqrt{s'}/\sqrt{s} > 0.10$, and a *non-radiative* sample, $\sqrt{s'}/\sqrt{s} > 0.85$; for muon and tau final states an *inclusive* sample, $\sqrt{s'} > 75$ GeV, and a *non-radiative* sample, $\sqrt{s'}/\sqrt{s} > 0.85$. For electron–positron final states, a cut on the

acollinearity [2] angle between the electron and positron, $\theta_{\mathrm{acol}} < 20°$, was applied, corresponding approximately to a cut of $\sqrt{s'} / \sqrt{s} > 0.85$.

The methods of estimating $\sqrt{s'}$ correspond to slightly different definitions of this variable. For $\mu^+\mu^-$ and the $\tau^+\tau^-$ final states, $\sqrt{s'}$ is the invariant mass of the muons or tau-leptons in the final state. For the inclusive hadronic final states, the estimated $\sqrt{s'}$ can be treated in theoretical predictions to be the invariant mass of the s-channel propagator.

For the e^+e^- final state the measured cross-sections and forward–backward asymmetries are for the electron and positron both within the acceptance $44° < \theta < 136°$. For the $\mu^+\mu^-$ and $\tau^+\tau^-$ final states, the cross-sections and asymmetries were extrapolated to 4π acceptance using samples of events generated with KORALZ [11]. In the calculations of KORALZ there is no interference between initial state and final state radiation. Corrections to the extrapolation for this interference were determined using the semi-analytical calculations of ZFITTER [12], in which the interference was computed to $\mathcal{O}(\alpha)$, and applied to the results. To account for missing higher order corrections, a systematic uncertainty of half the correction was taken. For the inclusive hadronic states, where the events are selected over the full solid angle, any correction for the interference between initial and final state radiation was estimated to be negligibly small compared to the precision of the measurement.

2.3. Improvements to analyses

The analyses of cross-sections for e^+e^-, $\mu^+\mu^-$, $\tau^+\tau^-$ and inclusive hadronic final states and forward–backward asymmetries for leptonic final states were similar to the ones performed at lower energies and the details, such as the event selection, and the determination of the reduced energy ($\sqrt{s'}$) can be found in [2], changes to each of the analyses are discussed below.

The distributions of $\sqrt{s'} / \sqrt{s}$ obtained for the real and the simulated data are shown in Fig. 1 for the muon, tau and inclusive hadronic channels for $\sqrt{s} \sim$ 189 GeV.

The numbers of events selected in the *inclusive* samples for each final state are given in Table 1. The efficiencies, the backgrounds from other channels and the backgrounds due to feed-up from the *inclusive* samples for the *non-radiative* event samples for each final states, are given in Table 2. Results are given in Section 2.5

2.3.1. Inclusive hadronic final states

A new cut was added. Events were only selected if their total transverse energy [3] was measured to be greater than 20% of the collision energy. This cut improves the rejection of two-photon collisions. The sum of the energies of the charged particles in an event was now required to be greater than 10% of the collision energy, relaxing the cut from the previous analysis.

The selection efficiencies and backgrounds were determined from simulated events. The four-fermion background was determined from events generated by PYTHIA [7] and EXCALIBUR [8]. The size of the background predicted by the two generators was found to be in good agreement; residual differences were taken into account in the systematic uncertainty on the measurement. The main background contributions to the cross-section measurement at 183 (189) GeV came from W-pair production with a contribution of 13.7 ± 0.3 pb $(14.7 \pm 0.3$ pb$)$ to the total cross-section and 8.3 ± 0.2 pb $(8.9 \pm 0.2$ pb$)$ to the non-radiative cross-section. The combined production of Z-pair and Ze^+e^- events was expected to contribute 2.8 ± 0.5 pb $(3.4 \pm 0.5$ pb$)$ to the total cross-section and 0.8 ± 0.3 pb $(1.1 \pm 0.2$ pb$)$ to the non-radiative event sample. Using samples of events generated with the TWOGAM [9] and BDKRC [10] generators, two-photon collisions were found to contribute significantly only to the total cross-section

---

[2] The acollinearity angle between two particles is defined as $\cos\theta_{\mathrm{acol}} = -\mathbf{p}_1 \cdot \mathbf{p}_2 / |\mathbf{p}_1||\mathbf{p}_2|$ where $\mathbf{p}_1$ and $\mathbf{p}_2$ are the 3-momenta of the particles.

[3] The total transverse energy is defined as $E_T = \Sigma E_i |\sin\theta_i|$ where E_i is the energy and θ_i is the polar angle of the ith particle in the event. DELPHI uses a right handed coordinate system in which the z axis is in the direction of the incoming electrons.
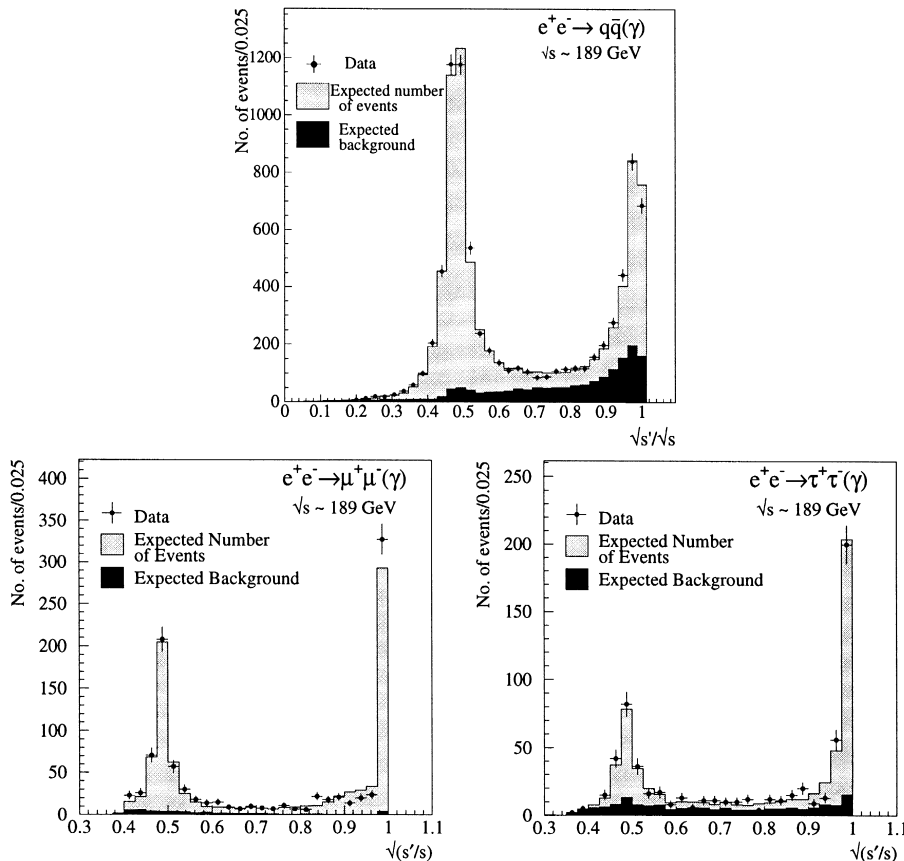
DELPHI

Fig. 1. Distributions of the reconstructed reduced energy for the $e^+e^- \to \mu^+\mu^-(\gamma)$, $e^+e^- \to \tau^+\tau^-(\gamma)$ and $e^+e^- \to q\bar{q}(\gamma)$ processes at $\sqrt{s} \sim 189$ GeV. The points stand for the data and the histograms represent the signal and background. The expected signals are simulated with the KORALZ generator [11] for the $e^+e^- \to \mu^+\mu^-(\gamma)$ and $e^+e^- \to \tau^+\tau^-(\gamma)$, and with PYTHIA generator [7] for the $e^+e^- \to q\bar{q}(\gamma)$ channel. The generator predictions were scaled to the ZFITTER [12] predictions for the total cross-sections and are normalised to the luminosities of the data sets analysed.

measurement for which there remains 1.8 ± 0.2 pb after event selection cuts at both 183 and 189 GeV.

Table 1
The numbers of events used in the analyses of the different final states. For each channel, the values refer to the samples with $\sqrt{s'/s} > 0.10$ for hadrons, $\sqrt{s'} > 75$ for muon and tau pairs and $\theta_{\mathrm{acol}} < 20°$ for electron–positron pairs

Channel	Energy (GeV)	
	~ 183	~ 189
$e^+e^- \to q\bar{q}(\gamma)$	5806	15726
$e^+e^- \to e^+e^-(\gamma)$	1109	2804
$e^+e^- \to \mu^+\mu^-(\gamma)$	354	974
$e^+e^- \to \tau^+\tau^-(\gamma)$	253	632

2.3.2. e^+e^- final states

In [2] results were presented for two different cuts on the acollinearity angle between the electron and positron, $\theta_{\mathrm{acol}} < 90°$ and $\theta_{\mathrm{acol}} < 20°$. In this paper, results are given for $\theta_{\mathrm{acol}} < 20°$ only, which is the sample with the highest sensitivity to the models of physics beyond the Standard Model considered in this paper.

2.3.3. $\mu^+\mu^-$ final states

Two improvements were made for the analysis of the data collected at $\sqrt{s} \sim 189$ GeV. The significant increase in the luminosity at this energy made it possible to measure the efficiency of the track recon-

Table 2
The efficiency, backgrounds and feed-up from the inclusive samples in the non-radiative samples of events selected in each of the channels

Channel	Energy (GeV)	Efficiency (%)	Background (%)	Feed-up (%)
$e^+e^- \to q\bar{q}$	~ 183	92.6	30.6	10.5
	~ 189	92.6	33.2	10.5
$e^+e^- \to e^+e^-$	~ 183	96.8	0.2	0.8
	~ 189	97.9	0.2	0.8
$e^+e^- \to \mu^+\mu^-$	~ 183	89.0	1.0	1.8
	~ 189	92.3	0.5	2.2
$e^+e^- \to \tau^+\tau^-$	~ 183	52.2	14.2	5.6
	~ 189	53.2	15.5	6.2

struction and muon identification efficiency from the data, exploiting the nearly back-to-back topology of the events with $\sqrt{s'}/\sqrt{s} > 0.85$ rather than relying on the efficiency determined from simulated events.

To do this, a sample of events with a high momentum muon was selected. The efficiency was then determined from the number of these events which did, or did not, contain a second reconstructed track or identified muon. The uncertainty on the combined track reconstruction and muon identification efficiency determined in this manner was $\pm 1.0\%$. The difference between the efficiency determined directly from simulation and that derived from the data at $\sqrt{s} \sim 189$ GeV was $\sim 2\%$. The efficiency determined from the simulation at $\sqrt{s} \sim 183$ GeV was corrected down by the $\sim 2\%$ difference measured at 189, and a systematic uncertainty of $\pm 2\%$ was applied to the results at $\sqrt{s} \sim 183$ GeV.

The polar angular coverage was extended from $20° < \theta < 160°$ to $14° < \theta < 164°$, taking advantage

of the increased luminosity to perform checks of the tracking and muon identification efficiency at extreme polar angles.

The background coming from four-fermion final states, via W^+W^-, ZZ and $Z\gamma^*$ production, was estimated from events generated by EXCALIBUR. The background from two-photon collisions was estimated from events generated using BDKRC.

2.3.4. $\tau^+\tau^-$ final states

There were several small improvements to the analysis of the $e^+e^- \to \tau^+\tau^-(\gamma)$ process. The acollinearity cut was placed at $0.3°$ instead of $0.5°$. Events with less than or equal to three charged particles in each hemisphere were included in the event selection (in addition to the events with only one charge particle in one hemisphere and less less than six charged particles in the other hemisphere) provided that the reconstructed invariant mass in each hemisphere was less than 2 GeV/c^2, consistent

Table 3
Systematic uncertainties of the total and non-radiative cross-section and forward–backward asymmetry measurements for the different final states. ''Non-radiative'' refers to $\sqrt{s'}/\sqrt{s} > 0.85$ for muon, tau and hadronic final states, and $\theta_{acol} < 20°$ for electron–positron pairs. ''Inclusive'' refers to $\sqrt{s'}/\sqrt{s} > 0.10$ for the hadronic final states and to $\sqrt{s'} > 75$ GeV for the muon and tau final states

	$\sqrt{s}$ (GeV)	$\Delta\sigma^h/\sigma^h$ (%)	$\Delta\sigma^e/\sigma^e$ (%)	$\Delta\sigma^\mu/\sigma^\mu$ (%)	$\Delta\sigma^\tau/\sigma^\tau$ (%)	ΔA_{FB}^e (10^{-3})	ΔA_{FB}^μ (10^{-3})	ΔA_{FB}^τ (10^{-3})
Non-radiative	~ 183	1.6	1.0	2.5	2.9	$^{+10}_{-3}$	4	16
	~ 189	1.8	1.0	1.7	3.0	$^{+10}_{-3}$	3	15
Inclusive	~ 183	1.1	–	2.5	3.8	–	2	16
	~ 189	1.1	–	1.4	4.1	–	2	15

with being the decay products of τ lepton. Both these changes improve the efficiency for the signal while not significantly increasing the levels of background.

The backgrounds were, as far as possible, estimated from the data by studying samples of events failing the specific cuts designed for rejection of a given background final state. The total systematic uncertainties on the cross-section and forward–backward asymmetry measurements for the different collision energies and channels are shown in Table 3.

In the determination of the forward–backward charge asymmetry of the τ leptons, the scattering angle was taken as the polar angle of the highest momentum charged particle in the hemisphere determined to have originated from the negatively charged τ lepton. The asymmetry was corrected for acceptance, background and for contamination due to radiative events from lower $\sqrt{s'}$ values. The determined asymmetries and the associated uncertainties are given in Tables 4 and 3 for the different centre-of-mass energies.

2.4. Differential cross-sections

In addition to the measurements of the cross-sections and asymmetries, measurements of the differential cross-sections, $d\sigma/d\cos\theta$, are given for the $\mu^+\mu^-$ and $\tau^+\tau^-$ final states for the *non-radiative* samples.

Fig. 2 shows the numbers of events observed in bins of $\cos\theta$ compared to simulations for each final state and each collision energy. For the $\mu^+\mu^-$ final states the scattering angle θ is the angle of the negative fermion with respect to the incoming electron in the laboratory frame, for the $\tau^+\tau^-$ final states the angle was defined in the same way as mentioned above for the measurement of the forward–backward asymmetry. Results are given in Section 2.5

2.5. Results of analyses

The results of the cross-section and asymmetry measurements are presented in Table 4 together with theoretical predictions. The errors indicated are statistical only. Systematic errors due to the event

Table 4

Results of the cross-section and asymmetry measurements for the different final states. The errors indicated are statistical only. Systematic errors related to the event selection and residual backgrounds are provided in Table 3. Those coming from the luminosity determination are given in the text. The hadronic, muon and tau results are corrected for all cuts, apart from the $\sqrt{s'}$ cut

		Energy (GeV)	
		~ 183	~ 189
σ_{had} (pb)	$\sqrt{s'}/\sqrt{s} > 0.85$	25.8 ± 0.8	22.1 ± 0.5
	theory	23.8	21.7
	$\sqrt{s'}/\sqrt{s} > 0.10$	107.8 ± 1.7	97.1 ± 1.0
	theory	106.0	97.4
$\sigma_{\mu\mu}$ (pb)	$\sqrt{s'}/\sqrt{s} > 0.85$	3.58 ± 0.28	3.04 ± 0.15
	theory	3.31	3.08
	$\sqrt{s'} > 75\,\text{GeV}$	8.92 ± 0.47	7.34 ± 0.24
	theory	7.69	7.15
$\sigma_{\tau\tau}$ (pb)	$\sqrt{s'}/\sqrt{s} > 0.85$	3.48 ± 0.39	3.21 ± 0.22
	theory	3.39	3.16
	$\sqrt{s'} > 75\,\text{GeV}$	9.12 ± 0.73	7.35 ± 0.39
	theory	7.73	7.18
A_{FB}^{μ}	$\sqrt{s'}/\sqrt{s} > 0.85$	0.565 ± 0.067	0.582 ± 0.041
	theory	0.594	0.588
	$\sqrt{s'} > 75\,\text{GeV}$	0.289 ± 0.051	0.362 ± 0.032
	theory	0.317	0.308
A_{FB}^{τ}	$\sqrt{s'}/\sqrt{s} > 0.85$	0.679 ± 0.082	0.693 ± 0.051
	theory	0.594	0.587
	$\sqrt{s'} > 75\,\text{GeV}$	0.296 ± 0.081	0.420 ± 0.050
	theory	0.316	0.315
σ_{ee} (pb)	$\theta_{\text{acol}} < 20°$	25.6 ± 0.8	22.6 ± 0.4
	theory	24.7	23.1
A_{FB}^{e}	$\theta_{\text{acol}} < 20°$	0.814 ± 0.017	0.810 ± 0.010
	theory	0.820	0.821

selection and to the residual background subtraction are shown in Table 3. For the cross-section measurements, they must be added in quadrature to the uncertainty coming from the luminosity determination. The theoretical predictions in Table 4 are from the TOPAZ0 program [13] for electron–positron final states and ZFITTER program [12] for the other final states. The uncertainties on the theoretical predictions are estimated to be below 1%.
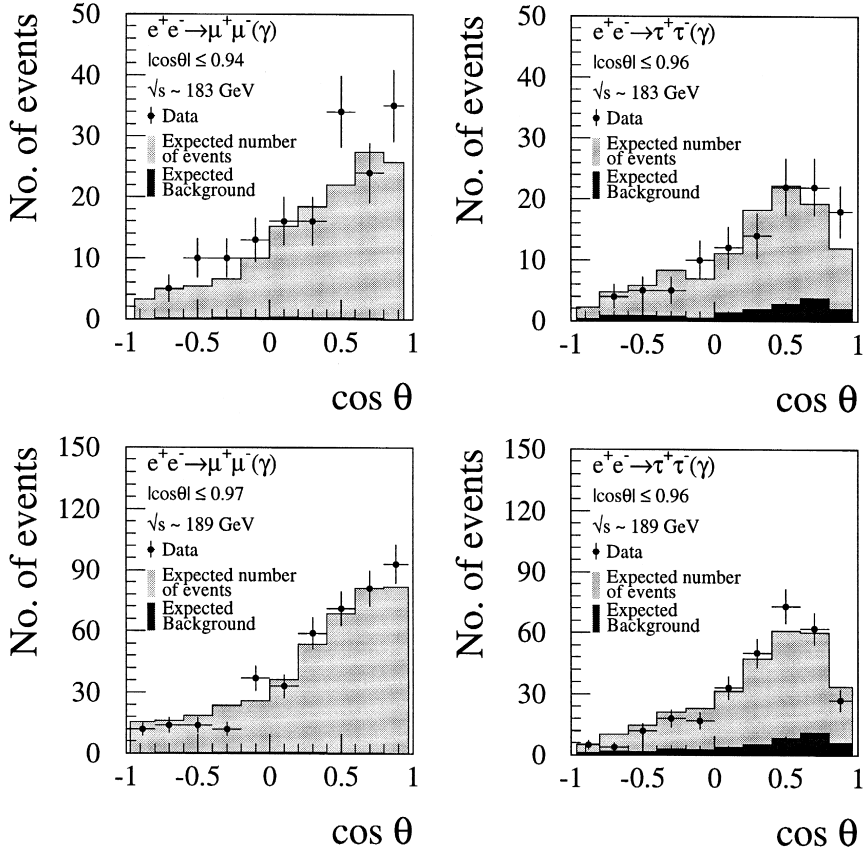
DELPHI

Fig. 2. The numbers of events observed as a function of $\cos\theta$ for $\mu^+\mu^-$ and $\tau^+\tau^-$ final states at centre-of-mass energies of ~ 183 and 189 GeV. The points stand for the data and the histograms represent the signal and background. The expected signals are simulated with the KORALZ [11] generator scaled to the ZFITTER [12] predictions and normalised to the luminosities of the data sets analysed.

Some components of the systematic uncertainties are correlated between measurements in different channels and different energies. This is the case for the theoretical uncertainty on the luminosity determination which is correlated between all cross-section measurements at all energies. For the $\mu^+\mu^-$ final states, the uncertainty on the event selection efficiency is correlated between energy points. The uncertainty on the extrapolation to 4π acceptance coming from the interference between initial and final state radiation is correlated between $\mu^+\mu^-$ and $\tau^+\tau^-$ final states and between energies. Given the

estimated size of the correlations compared to the precision of the measurements these correlations are ignored.

Fig. 3 shows the measured hadron, electron–positron pair, muon-pair and tau-pair cross-sections for all collision energies ranging from 130 up to 189 GeV from DELPHI. The forward–backward asymmetries for electron–positron pairs, muon-pairs and tau-pairs are shown in Fig. 4.

The results of the analyses of the differential cross-sections for $\mu^+\mu^-$ and $\tau^+\tau^-$ final states are tabulated, including statistical and systematic errors,

in Table 5. The theoretical predictions are from the ZFITTER program, and have an uncertainty estimated to be below 1%.

For the $e^+e^- \to \mu^+\mu^-$ channel the systematic errors quoted in Table 5 include correlated systematic uncertainties of 2% for the data at $\sqrt{s} \sim 183\,\text{GeV}$ and 1% for the data at $\sqrt{s} \sim 189\,\text{GeV}$ in the measured cross-sections for all bins of $\cos\theta$ arising from the determination of the track reconstruction and muon identification efficiencies which were applied as an overall correction to the efficiencies determined bin by bin in $\cos\theta$ from simulated events.
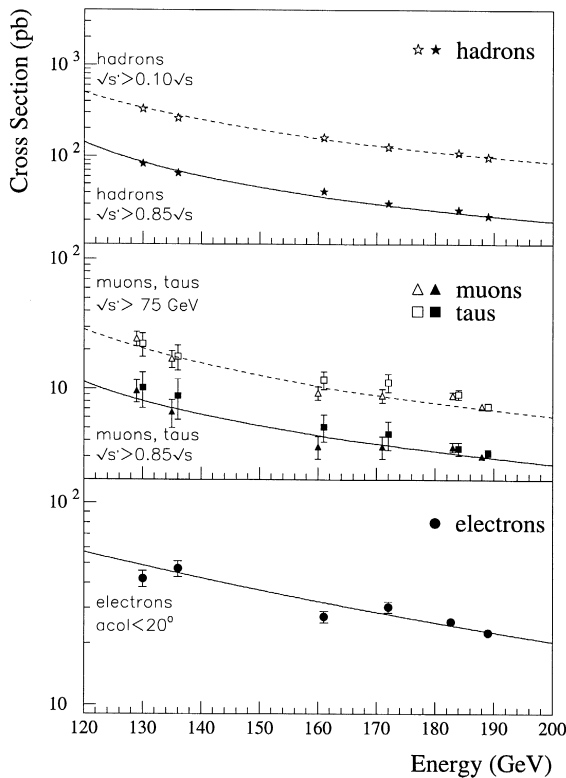
DELPHI

Fig. 3. Cross-sections for the $e^+e^- \to q\bar{q}(\gamma)$, $\mu^+\mu^-(\gamma)$ and $\tau^+\tau^-(\gamma)$ and $e^+e^- \to e^+e^-(\gamma)$ processes measured at energies from 130 up to 189 GeV. The curves show the SM prediction of the TOPAZ0 program [13] for electron–positron final states and ZFITTER program [12] for the other final states. Solid points and solid lines represent the *non-radiative* selections, open points and dashed lines represent the *inclusive* selections.
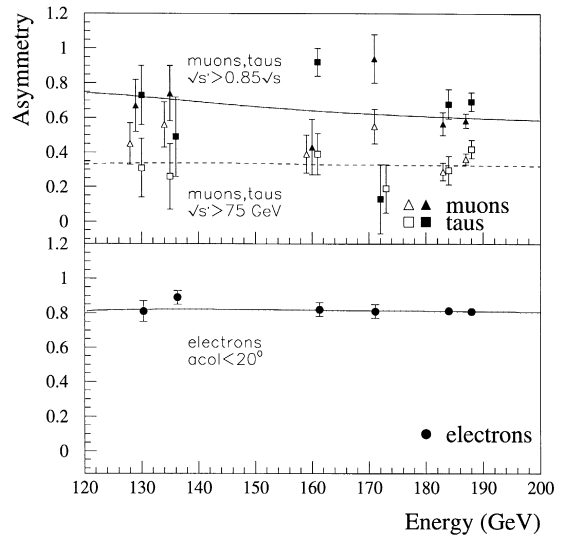
DELPHI

Fig. 4. The forward–backward charge asymmetries in the reactions $e^+e^- \to \mu^+\mu^-(\gamma)$, $\tau^+\tau^-(\gamma)$ and $e^+e^-(\gamma)$ measured at energies ranging from 130 to 189 GeV. The curves show the SM prediction of the TOPAZ0 program [13] for electron–positron final states and ZFITTER program [12] for the other final states. Solid points and solid lines represent the *non-radiative* selections, open points and dashed lines represent the *inclusive* selections.

Overall, no substantial departure of the measurements of fermion-pair production from the Standard Model predictions was found.

3. Physics beyond the Standard Model

The data presented in this paper were used to improve the constraints on physics beyond the Standard Model given in Section 6 of [2] for three sets of models: contact interactions between leptons, models including Z′ bosons and R-parity violating sneutrino exchange. The theoretical bases of each of these models are discussed in Section 5 of [2], the key points are summarised below. New limits for models which include gravity in extra dimensions are derived from the measurements of the differential cross-sections given in this paper. Unless otherwise stated the systematic errors on the measurements at LEP II energies have been added in quadrature with

Table 5

The differential cross-sections for non-radiative $\mu^+\mu^-$ and $\tau^+\tau^-$ final states at centre-of-mass energies of ~ 183 and 189 GeV. The errors shown are respectively the statistical and systematic components. The Standard Model expectations (SM) were computed with the ZFITTER program [12]

	$\cos\theta$	$d\sigma / d\cos\theta$ (pb)	
		theory	measurement
$e^+e^- \to \mu^+\mu^-$	$[-0.94, -0.80]$	0.478	$0.000 \pm 0.178 \pm 0.013$
($\sqrt{s} \sim 183$ GeV)	$[-0.80, -0.60]$	0.486	$0.514 \pm 0.230 \pm 0.013$
	$[-0.60, -0.40]$	0.576	$0.989 \pm 0.313 \pm 0.024$
	$[-0.40, -0.20]$	0.761	$0.972 \pm 0.307 \pm 0.023$
	$[-0.20, 0.00]$	1.045	$1.298 \pm 0.360 \pm 0.032$
	$[0.00, 0.20]$	1.428	$1.591 \pm 0.398 \pm 0.039$
	$[0.20, 0.40]$	1.913	$1.605 \pm 0.401 \pm 0.039$
	$[0.40, 0.60]$	2.503	$3.377 \pm 0.579 \pm 0.081$
	$[0.60, 0.80]$	3.206	$2.466 \pm 0.503 \pm 0.061$
	$[0.80, 0.94]$	4.078	$4.978 \pm 0.841 \pm 0.119$
$e^+e^- \to \tau^+\tau^-$	$[-0.96, -0.80]$	0.49	$-0.13 \pm 0.24 \pm 0.04$
($\sqrt{s} \sim 183$ GeV)	$[-0.80, -0.60]$	0.50	$0.48 \pm 0.31 \pm 0.04$
	$[-0.60, -0.40]$	0.60	$0.52 \pm 0.28 \pm 0.04$
	$[-0.40, -0.20]$	0.79	$0.56 \pm 0.30 \pm 0.04$
	$[-0.20, 0.00]$	1.08	$1.62 \pm 0.54 \pm 0.12$
	$[0.00, 0.20]$	1.48	$1.56 \pm 0.51 \pm 0.12$
	$[0.20, 0.40]$	1.97	$1.65 \pm 0.51 \pm 0.12$
	$[0.40, 0.60]$	2.58	$2.49 \pm 0.61 \pm 0.19$
	$[0.60, 0.80]$	3.31	$3.91 \pm 1.00 \pm 0.29$
	$[0.80, 0.96]$	4.08	$6.77 \pm 1.80 \pm 0.50$
$e^+e^- \to \mu^+\mu^-$	$[-0.97, -0.80]$	0.465	$0.495 \pm 0.143 \pm 0.008$
($\sqrt{s} \sim 189$ GeV)	$[-0.80, -0.60]$	0.467	$0.478 \pm 0.128 \pm 0.008$
	$[-0.60, -0.40]$	0.546	$0.448 \pm 0.120 \pm 0.007$
	$[-0.40, -0.20]$	0.713	$0.391 \pm 0.113 \pm 0.006$
	$[-0.20, 0.00]$	0.971	$1.287 \pm 0.212 \pm 0.021$
	$[0.00, 0.20]$	1.322	$1.129 \pm 0.197 \pm 0.018$
	$[0.20, 0.40]$	1.769	$1.908 \pm 0.248 \pm 0.029$
	$[0.40, 0.60]$	2.315	$2.445 \pm 0.290 \pm 0.039$
	$[0.60, 0.80]$	2.968	$2.927 \pm 0.325 \pm 0.048$
	$[0.80, 0.97]$	3.780	$3.986 \pm 0.413 \pm 0.065$
$e^+e^- \to \tau^+\tau^-$	$[-0.96, -0.80]$	0.48	$0.58 \pm 0.34 \pm 0.05$
($\sqrt{s} \sim 189$ GeV)	$[-0.80, -0.60]$	0.48	$0.12 \pm 0.13 \pm 0.03$
	$[-0.60, -0.40]$	0.56	$0.48 \pm 0.16 \pm 0.04$
	$[-0.40, -0.20]$	0.73	$0.67 \pm 0.19 \pm 0.05$
	$[-0.20, 0.00]$	1.00	$0.75 \pm 0.22 \pm 0.06$
	$[0.00, 0.20]$	1.37	$1.57 \pm 0.31 \pm 0.13$
	$[0.20, 0.40]$	1.83	$2.05 \pm 0.32 \pm 0.16$
	$[0.40, 0.60]$	2.39	$2.96 \pm 0.39 \pm 0.23$
	$[0.60, 0.80]$	3.06	$3.26 \pm 0.51 \pm 0.26$
	$[0.80, 0.96]$	3.78	$2.87 \pm 0.71 \pm 0.24$

the statistical errors treating them as uncorrelated between measurements.

3.1. Contact interaction models

Contact interactions between fermions can be parameterised as an effective Lagrangian with the form:

$$\mathscr{L}_{\text{eff}} = \frac{g^2}{(1+\delta)\,\Lambda^2} \sum_{i,j=L,R} \eta_{ij}\,\bar{e}_i\gamma_\mu e_i \bar{f}_j\gamma^\mu f_j. \qquad (1)$$

where Λ is the characteristic energy scale of the interactions. Different choices of η_{ij} lead to 12 commonly studied models, referred to as LL, RR, etc. [14].

Fits were made using data at all energies from 130 to 189 GeV for $e^+e^- \to e^+e^-$, $e^+e^- \to \mu^+\mu^-$, $e^+e^- \to \tau^+\tau^-$ channels and $e^+e^- \to l^+l^-$, a combination of all leptonic final states assuming lepton universality. The parameter fitted was $\epsilon = 1/\Lambda^2$. The values of ϵ extracted for each model were all compatible with the Standard Model expectation $\epsilon = 0$, at the two standard deviation level. The errors on ϵ in the $e^+e^- \to l^+l^-$ fit are typically 30% smaller than those reported in [2] as a result of the inclusion of the data collected at $\sqrt{s} \sim 183$ and 189 GeV. The fitted values of ϵ were converted into lower limits on Λ at 95% confidence level. The results are given in Table 6.

3.2. Sneutrino exchange

The second set of models consider possible s or t channel sneutrino ($\nu_{\tilde{\ell}}$) exchange in R-parity violating supersymmetry [15]. The parameters of interest are the dimensionless couplings, λ_{ijk}, between the superfields of different generations, i, j and k, together with the mass of the sneutrino exchanged, $m_{\tilde{\nu}}$. The sneutrino width is not constrained within R-parity violating supersymmetry; a value of 1 GeV has been used [15].

For the $e^+e^- \to \mu^+\mu^-$ and $e^+e^- \to \tau^+\tau^-$ channels, in the case that only one λ value is non-zero there would only be t-channel sneutrino effects. The 95% confidence exclusion upper limits on λ are given in Table 7, assuming sneutrino masses of either 100 or 200 GeV/c^2. The limits are calculated by finding the value of λ for $\chi^2 = \chi^2_{\min} + 3.84$. The limits are between 0.02 and 0.14 lower than those published in [2] depending on the channel and the mass assumed.

Table 6

Fitted values of ϵ and 95% confidence lower limits on the scale, Λ, of contact interactions in the models discussed in the text, for $e^+e^- \rightarrow e^+e^-$, $e^+e^- \rightarrow \mu^+\mu^-$, $e^+e^- \rightarrow \tau^+\tau^-$ final states and also for $e^+e^- \rightarrow l^+l^-$ in which lepton universality is assumed for the contact interactions. The errors on ϵ are statistical only. The models are defined in [14]

	Model	$\epsilon^{+\sigma_+}_{-\sigma_-}$ (TeV^{-2})	Λ^+ (TeV)	Λ^- (TeV)
$e^+e^- \rightarrow e^+e^-$	LL	$0.016^{+0.022}_{-0.020}$	4.4	5.4
	RR	$0.016^{+0.023}_{-0.020}$	4.3	5.3
	VV	$0.002^{+0.005}_{-0.004}$	9.8	11.7
	AA	$0.007^{+0.010}_{-0.014}$	6.6	7.1
	RL	$0.003^{+0.018}_{-0.013}$	5.5	6.3
	LR	$0.003^{+0.018}_{-0.013}$	5.5	6.3
$e^+e^- \rightarrow \mu^+\mu^-$	LL	$-0.002^{+0.013}_{-0.014}$	6.6	6.3
	RR	$-0.002^{+0.014}_{-0.016}$	6.3	5.9
	VV	$0.001^{+0.004}_{-0.006}$	10.9	10.1
	AA	$-0.003^{+0.009}_{-0.005}$	9.1	9.2
	RL	$-0.252^{+0.261}_{-0.016}$	2.1	1.9
	LR	$-0.252^{+0.261}_{-0.016}$	2.1	1.9
$e^+e^- \rightarrow \tau^+\tau^-$	LL	$0.004^{+0.020}_{-0.022}$	5.2	5.4
	RR	$0.004^{+0.023}_{-0.023}$	4.9	5.1
	VV	$-0.011^{+0.009}_{-0.006}$	9.0	7.0
	AA	$0.019^{+0.012}_{-0.009}$	5.1	7.8
	RL	$-0.163^{+0.100}_{-0.049}$	2.9	2.0
	LR	$-0.163^{+0.100}_{-0.049}$	2.9	2.0
$e^+e^- \rightarrow l^+l^-$	LL	$0.005^{+0.009}_{-0.011}$	7.3	7.8
	RR	$0.004^{+0.011}_{-0.010}$	6.8	7.6
	VV	$0.001^{+0.002}_{-0.004}$	14.5	12.7
	AA	$0.006^{+0.005}_{-0.005}$	8.3	10.9
	RL	$-0.008^{+0.010}_{-0.011}$	7.6	6.2
	LR	$-0.008^{+0.010}_{-0.011}$	7.6	6.2

For the $e^+e^- \rightarrow e^+e^-$ channel the resulting 95% limits on λ, are given in Fig. 5(a), as a function of $m_{\tilde{\nu}}$. For the fits in the $e^+e^- \rightarrow \mu^+\mu^-$ channel, as-

Table 7

Upper limits on the couplings λ in t channel sneutrino exchange in $e^+e^- \rightarrow \mu^+\mu^-$ and $e^+e^- \rightarrow \tau^+\tau^-$ for sneutrino masses of 100 and 200 GeV/c^2. The couplings involved are given in the text

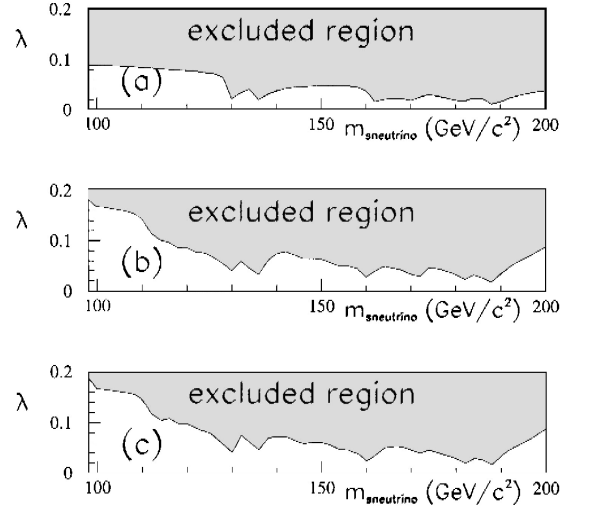| Coupling	$m_{\tilde{\nu}} = 100\,\text{GeV}/c^2$ (95% C.L.)	$m_{\tilde{\nu}} = 200\,\text{GeV}/c^2$ (95% C.L.)
λ (t-chann. $\nu_{\tilde{\ell}}$ in $e^+e^- \rightarrow \mu^+\mu^-$)	0.50	0.68
λ (t-chann. $\nu_{\tilde{\ell}}$ in $e^+e^- \rightarrow \tau^+\tau^-$)	0.47	0.65

DELPHI

Fig. 5. The 95% exclusion limits for (a) λ_{121} (or λ_{131}), as a function of $m_{\tilde{\nu}}$, obtained from the $e^+e^- \rightarrow e^+e^-$ channel; (b) $\lambda_{131} = \lambda_{232} = \lambda$, as a function of $m_{\tilde{\nu}}$, obtained from the $e^+e^- \rightarrow \mu^+\mu^-$ channel; (c) $\lambda_{121} = \lambda_{233} = \lambda$, as a function of $m_{\tilde{\nu}}$, obtained from the $e^+e^- \rightarrow \tau^+\tau^-$ channel. The sneutrino width is taken to be 1 GeV.

suming that $\lambda_{131} = \lambda_{232} = \lambda$, the resulting 95% limits on λ are given in Fig. 5(b). The exclusion contour for $\lambda_{121} = \lambda_{233} = \lambda$, using the $e^+e^- \rightarrow \tau^+\tau^-$ channel, is shown in Fig. 5(c). In each case, the exclusion contours are calculated by finding the value of λ for $\chi^2 = \chi^2_{\text{min}} + 3.84$ for each value of $m_{\tilde{\nu}}$ separately. A coupling of $\lambda > 0.1$ can be excluded for $m_{\tilde{\nu}}$ in the range 130–190 GeV/c^2 for all final states, extending the excluded region by approximately 20 GeV/c^2 compared to [2].

3.3. Z′-bosons

Existing data from LEP1 and LEP2 and the cross-sections and asymmetries given here were used to fit the data to models including additional Z′ bosons.

3.3.1. Model dependent fits

Fits were made to the mass of a Z′, $M_{Z'}$, the mass of the Z, M_Z, and to the mixing angle between the two bosonic fields, $\Theta_{ZZ'}$, for 4 different models

referred to as χ, ψ, η and L–R [16]. The theoretical prediction made came from the ZEFIT package [18]. The fitted value of M_Z was found to be in agreement with the value found from fits to the data with no additional Z′. No evidence was found for the existence of a Z′-boson in any of the models. The 95% confidence level limits on $M_{Z'}$, and $\Theta_{ZZ'}$, were computed for the different model by determining the contours of the domain in the $M_{Z'} - \Theta_{ZZ'}$ plane where $\chi^2 < \chi^2_{\min} + 5.99$ [19]. The allowed regions for $M_{Z'}$ and $\Theta_{ZZ'}$ are shown in Fig. 6. The lower limits, shown in Table 8, on the Z′ mass range from 310 to 440 GeV/c^2, an increase of between 70 and 190 GeV/c^2 on the limits presented in [2], depending on the model.

In addition to the models considered in [2] a limit has been obtained on the mass and mixing of the Z′ in the Sequential Standard Model [20]. This model proposes the existence of a Z′ with exactly the same coupling to fermions as the standard Z. A limit of $M_{Z'} > 710 \, \text{GeV}/c^2$ is found at 95% confidence level.

3.3.2. Model independent fits

Model Independent fits were performed to the leptonic cross-sections and forward–backward asym-
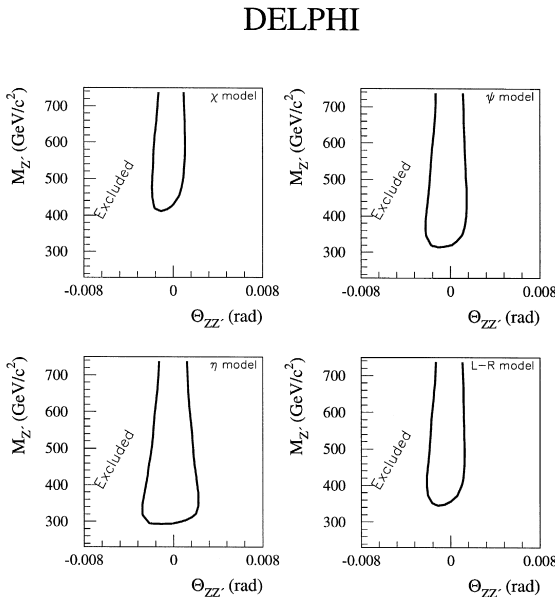
DELPHI

Fig. 6. The allowed domain in the $M_{Z'} - \Theta_{ZZ'}$ plane for the χ, ψ, η and L–R models [16]. The contours show the 95% confidence level limits.

Table 8
95% confidence level lower limits on the Z′ mass and upper limits on the ZZ′ mixing angle within the χ, ψ, η and L–R models [16]

	Model			
	χ	ψ	η	L–R
M_Z^{limit} (GeV/c^2)	440	350	310	380
$\|\Theta_{ZZ'}^{\text{limit}}\|$ (radians)	0.0017	0.0018	0.0024	0.0018

metries, for the leptonic couplings of a Z′, $a_{l'}^N$ and $v_{l'}^N$, normalised for the overall coupling scale and the mass of the Z′ [17].

Several values of the mass of the Z′ were considered (i.e. 300, 500 and 1000 GeV/c^2), and the ZZ′-mixing was neglected. The limits on the normalised couplings are $|a_{l'}^N| < 0.15$ and $|v_{l'}^N| < 0.22$, a decrease of 0.04 and 0.22, respectively, on limits given in [2].

3.4. Gravity in extra dimensions

The large difference between the electroweak scale ($M_{EW} \sim 10^2 - 10^3$ GeV) and the scale at which quantum gravitational effects become strong, the Planck scale ($M_{Pl} \sim 10^{19}$ GeV), leads to the well known ''hierarchy problem''. A solution, not relying on supersymmetry or technicolour, has been proposed [21] that involves an effective Planck scale, M_D, of $\mathscr{O}$(TeV). This is achieved by introducing n compactified dimensions, into which spin 2 gravitons propagate, in addition to the 4 dimensions of standard space-time. The Planck mass seen in the 4 uncompactified dimensions, M_{Pl}, can be expressed in terms of M_D, the effective Planck scale in the $n + 4$ dimensional theory,

$$M_{Pl}^2 \sim R^n M_D^{n+2}$$

where R is the size of the extra dimensions. With $M_D = 1$ TeV, the case where $n = 1$ is excluded as Newtonian gravitation would be modified at solar system distances whereas, $n = 2$ corresponds to a radius for extra dimensions of $\mathscr{O}$(1 mm), which is not excluded by existing gravitational experiments [22].

In high energy collisions at LEP and other colliders, new channels not present in the Standard Model would be available in which gravitons could be produced or exchanged. Virtual graviton exchange

Table 9

95% confidence level lower limits on M_s in models of gravity in extra dimensions for $\mu^+\mu^-$ and $\tau^+\tau^-$ final states, and for l^+l^-, a combination of both muon and tau final states.

Final state	ϵ_{fit} (TeV^{-4})	λ	M_s(TeV) (95% C.L.)
$\mu^+\mu^-$	$-6.53^{+4.61}_{-2.24}$	-1	0.559
		$+1$	0.649
$\tau^+\tau^-$	$-10.91^{+3.84}_{-8.18}$	-1	0.450
		$+1$	0.564
l^+l^-	$-8.39^{+3.75}_{-1.96}$	-1	0.542
		$+1$	0.680

would affect the differential cross section for $e^+e^- \to f\bar{f}$, with the largest contributions seen at low angles with respect to the incoming electron or positron. Embedding the model into a string model, and identifying the effective Planck scale, M_D, with the string scale, M_s, the differential cross section for $e^+e^- \to f\bar{f}$ with the inclusion of the spin 2 graviton can be expressed as [23]:

$$\frac{d\sigma}{d\cos\theta} = A(\cos\theta) + B(\cos\theta)\left[\frac{\lambda}{M_s^4}\right]$$
$$+ C(\cos\theta)\left[\frac{\lambda}{M_s^4}\right]^2,$$

with θ being the polar angle of the outgoing fermion with respect to the direction of the incoming electron. The functions A, B and C are known, and the maximum power in the expansion is $\cos\theta^4$. The dimensionless parameter λ, of $\mathcal{O}(1)$, is not explicitly calculable without full knowledge of the underlying

quantum gravitational theory. It can be either positive or negative [23,24]. For the purposes of the fits, two cases, $\lambda = \pm 1$, are considered. This parameterisation has no explicit dependence on the number of extra dimensions, n.

Fits to the differential cross-sections, $d\sigma/d\cos\theta$, measured at $\sqrt{s} \sim 183$ and 189 GeV for the parameter $\epsilon = \lambda/M_s^4$ were performed, giving values compatible with the Standard Model, i.e. $\epsilon = 0$. The systematics errors known to be fully correlated between bins of $\cos\theta$ where treated as such. Table 9 shows the fitted values of ϵ and 95% confidence level lower limits on M_s. These limits were obtained using a method equivalent to that used to extract the limits on the scale, Λ, of contact interactions, as described in Section 6.1.1 of [2].

The angular distributions predicted at $\sqrt{s} \sim 189$ GeV for the fitted values of ϵ are shown in Fig. 7. The predictions for the values of M_s at the limits with $\lambda = \pm 1$, the data and the Standard Model predictions are superimposed.

4. Summary and conclusions

The results of the analyses of cross-sections and asymmetries in the channels $e^+e^- \to e^+e^-(\gamma)$, $e^+e^- \to \mu^+\mu^-(\gamma)$, $e^+e^- \to \tau^+\tau^-(\gamma)$ and inclusive $e^+e^- \to q\bar{q}(\gamma)$, at $\sqrt{s} \sim 183 - 189$ GeV have been presented. Overall, the data agree with the Standard
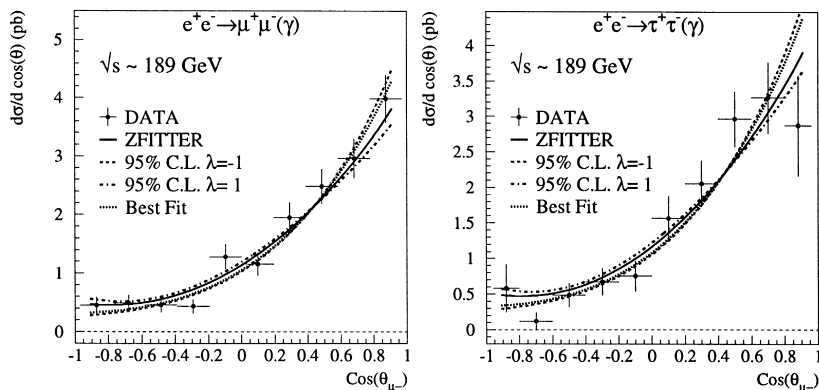

Fig. 7. Fits to angular distributions for $\mu^+\mu^-$ and $\tau^+\tau^-$ final states, for models which include gravity in extra dimensions. The dashed fitted curves correspond to $\epsilon = -8.39$ TeV^{-4}, the *best fit* to all data. The data are compared to the Standard Model predictions of ZFITTER and to the differential cross-sections predicted at 95% C.L. for $\lambda = \pm 1$.

Model predictions as calculated with ZFITTER and TOPAZ0. The data were used to update previous searches for physics beyond the Standard Model given and to investigate the possible effects of gravity in extra dimensions. No evidence for physics beyond the Standard Model was found and limits were set on parameters of several more general models. The scale Λ characterising contact interactions between leptons can be excluded at 95% confidence level in the range $\Lambda < 4.4 - 10.7$ TeV depending on the model. For sneutrino exchange in R-parity violating supersymmetry, the generic coupling in the purely leptonic part of the superpotential, $\lambda > 0.1$ can be excluded for $m_{\tilde{\nu}}$ in the range 130 - 190 GeV for all leptonic states at the 95% confidence level or above. Alternatively, Z' bosons lighter than $\sim$ 300 GeV/c^2 can be excluded at the 95% confidence level in the models considered. Lastly, 95% confidence level lower limits of 542 and 680 GeV on the string scale, M_s, in models of gravity involving extra dimensions are obtained for a combinations of $\mu^+\mu^-$ and $\tau^+\tau^-$ final states.

Acknowledgements

References

[1] DELPHI Collaboration, P. Aarnio et al., Nucl. Instr. & Meth. A 303 (1991) 233. DELPHI Collaboration, P. Abreu et al., Nucl. Instr. & Meth. A 378 (1996) 57.

[2] DELPHI Collaboration, P. Abreu et al., Eur. Phys. J. C 11 (1999) 383.

[3] DELPHI Collaboration, P. Abreu et al., Nucl. Phys. B 417 (1994) 3.

[4] DELPHI Collaboration, P. Abreu et al., Nucl. Phys. B 418 (1994) 403; DELPHI Collaboration, in preparation.

[5] ALEPH Collaboration, D. Buskulic et al., Phys. Lett. B 378 (1996) 373; ALEPH Collaboration, R. Barate et al., Phys. Lett. B 399 (1997) 329; ALEPH Collaboration, R. Barate et al., Eur. Phys. J. C 12 (2000) 183; L3 Collaboration, M. Acciarri et al., Phys. Lett. B 370 (1996) 195; L3 Collaboration, M. Acciarri et al., Phys. Lett. B 407 (1997) 361; L3 Collaboration, M. Acciarri et al., Phys. Lett. B 433 (1998) 163; L3 Collaboration, M. Acciarri et al., Phys. Lett. B 464 (1999) 135; L3 Collaboration, M. Acciarri et al., Phys. Lett. B 470 (1999) 281; L3 Collaboration, M. Acciarri et al., Phys. Lett. B 479 (2000) 101; OPAL Collaboration, K. Ackerstaff et al., Eur. Phys. J. C 2 (1998) 441; OPAL Collaboration, G. Abbiendi et al., Eur. Phys. J. C 6 (1999) 1; OPAL Collaboration, G. Abbiendi et al., Eur. Phys. J. C 13 (2000) 553.

[6] LEP Energy Working Group 99-01; CERN-EP-98-191.

[7] T. Sjöstrand, PYTHIA 5.7/JETSET 7.4 CERN-TH 7112/93, 1993.

[8] F.A. Berends, R. Pittau, R. Kliess, Comp. Phys. Comm. 85 (1995) 437.

[9] S. Nova et al., DELPHI Note 90-35.

[10] F.A. Berends, P.H. Daverveldt, R. Klies, Comp. Phys. Comm. 40 (1986) 271.

[11] S. Jadach, B.F.L. Ward, Z. Was, Comp. Phys. Comm. 79 (1994) 503.

[12] D. Bardin et al., ZFITTER: An Analytical Program for Fermion Pair Production in e^+e^- Annihilation, hep-ph/9908433.

[13] G. Montagna et al., Nucl. Phys. B 401 (1993) 3; G. Montagna et al., Comput. Phys. Commun. 76 (1993) 328.

[14] E. Eichten, K. Lane, M. Peskin, Phys. Rev. Lett. 50 (1983) 811.

[15] J. Kalinowski et al., Zeit. Phys. C 74 (1997) 595.

[16] P. Langacker, R.W. Robinett, J.L. Rosner, Phys. Rev. D 30 (1984) 1470; D. London, J.L. Rosner, Phys. Rev. D 34

(1986) 1530; J.C. Pati, A. Salam, Phys. Rev. D 10 (1974) 275; R.N. Mohapatra, J.C. Pati, Phys. Rev. D 11 (1975) 566.

[17] A. Leike, Zeit. Phys. C 62 (1994) 265.

[18] A. Leike, S. Riemann, T. Riemann, Munich University preprint LMU-91/6.

[19] F. James, MINUIT Reference Manual, CERN Program Library Long Writeup D 506 (1994).

[20] G. Altarelli et al., Z. Phys. C 45 (1989) 109; Z. Phys. C 47 (1990) 676 (E).

[21] N. Arkani-Hamed et al., Phys. Rev. D 59 (1999) 086004.

[22] J.C. Long et al., Nucl. Phys. B 539 (1999) 23.

[23] J.L. Hewett, Phys. Rev. Lett. 82 (1999) 4765.

[24] G.F. Giudice et al., Nucl. Phys. B 544 (1999) 3.